The Astrophysical Journal, 730:5 (12pp), 2011 March 20 doi:10.1088/0004-637X/730/1/5

EXTREME FEEDBACK AND THE EPOCH OF REIONIZATION: CLUES IN THE LOCAL UNIVERSE

Timothy M. Heckman[1], Sanchayeeta Borthakur[1], Roderik Overzier[2], Guinevere Kauffmann[2], Antara Basu-Zych[3], Claus Leitherer[4], Ken Sembach[4], D. Chris Martin[5], R. Michael Rich[6], David Schiminovich[7], and Mark Seibert[8]
[1] Center for Astrophysical Sciences, Department of Physics & Astronomy, Johns Hopkins University, Baltimore, MD 21218, USA; heckman@pha.jhu.edu
[2] Max-Planck-Institute for Astrophysics, Garching D-85741, Germany
[3] Goddard Space Flight Center, Greenbelt, MD 20771, USA
[4] Space Telescope Science Institute, Baltimore, MD 21218, USA
[5] Astronomy Department, Caltech, Pasadena, CA 91125, USA
[6] Department of Physics & Astronomy, UCLA, Los Angeles, CA 90095, USA
[7] Department of Astronomy, Columbia University, New York, NY 10027, USA
[8] Carnegie Institution of Washington Observatories, Pasadena, CA 91101, USA
Received 2010 November 17; accepted 2011 January 19; published 2011 February 23

ABSTRACT

The source responsible for reionizing the universe at $z > 6$ remains uncertain. While an energetically adequate population of star-forming galaxies may be in place, it is unknown whether a large enough fraction of their ionizing radiation can escape into the intergalactic medium. Attempts to measure this escape fraction in intensely star-forming galaxies at lower redshifts have largely yielded upper limits. In this paper, we present new *Hubble Space Telescope* Cosmic Origins Spectrograph and archival *Far-Ultraviolet Spectroscopic Explorer* (*FUSE*) far-UV spectroscopy of a sample of 11 Lyman Break Analogs (LBAs), a rare population of local galaxies that strongly resemble the high-z Lyman Break galaxies. We combine these data with Sloan Digital Sky Survey optical spectra and *Spitzer* photometry. We also analyze archival *FUSE* observations of 15 typical UV-bright local starbursts. We find evidence of small covering factors for optically thick neutral gas in three cases. This is based on two independent pieces of evidence: a significant residual intensity in the cores of the strongest interstellar absorption-lines tracing neutral gas and a small ratio of extinction-corrected Hα to UV plus far-IR luminosities. These objects represent three of the four LBAs that contain a young, very compact ($\sim 10^2$ pc), and highly massive ($\sim 10^9\ M_\odot$) dominant central object (DCO). These three objects also differ from the other galaxies in showing a significant amount of blueshifted Lyα emission, which may be related to the low covering factor of neutral gas. All four LBAs with DCOs in our sample show extremely high velocity outflows of interstellar gas, with line centroids blueshifted by about 700 km s^{-1} and maximum outflow velocities reaching at least 1500 km s^{-1}. We show that these properties are consistent with an outflow driven by a powerful starburst that is exceptionally compact. We speculate that such extreme feedback may be required to enable the escape of ionizing radiation from star-forming galaxies.

Key words: galaxies: evolution – galaxies: high-redshift – galaxies: ISM – galaxies: kinematics and dynamics – intergalactic medium

1. INTRODUCTION

Following the epoch of recombination at $z \sim 1000$, the next major event in the history of the universe was its reionization by an early generation of massive stars and/or black holes. One of the major goals of modern cosmology is to understand this process: what sources were responsible and when did it occur? Observations of the cosmic microwave background with *WMAP* show that reionization occurred at a mean redshift of 11.0 ± 1.4 (Dunkley et al. 2009), while observations of absorption due to the Lyα forest in quasars show that reionization was not quite complete until a redshift of about six (e.g., Fan et al. 2006).

Based on the observed luminosity functions of active galactic nuclei (AGNs) and star-forming galaxies at the relevant redshifts, the latter appear to be the more energetically plausible source for reionization (e.g., Bouwens et al. 2010). However, a major uncertainty in the contribution of star-forming galaxies is the poorly constrained fraction of ionizing photons that are able to leak out of such galaxies into the intergalactic medium. Bouwens et al. (2010) estimate that an escape fraction of 20% (60%) is required for consistency with the *WMAP* results at the 2σ (1σ) level. This is much higher than the escape fraction of 1–2% measured for the Milky Way (Putman et al. 2003).

Many attempts have been made to measure this escape fraction in other star-forming galaxies at low redshift (Leitherer et al. 1995; Hurwitz et al. 1997; Deharveng et al. 2001; Heckman et al. 2001, hereafter H01; Bergvall et al. 2006; Grimes et al. 2009, hereafter G09), intermediate redshift (Malkan et al. 2003; Siana et al. 2007, 2010; Cowie et al. 2009), and high redshift (Steidel et al. 2001; Giallongo et al. 2002; Fernandez-Soto et al. 2003; Inoue et al. 2005; Vanzella et al. 2010). For the most part, these measurements have only yielded upper limits, although significant escaping Lyman continuum emission has been detected in 17 out of a sample of 198 Lyman Break and Lyα galaxies at $z > 3$ (Iwata et al. 2009), consistent with earlier results for a smaller sample of Lyman Break galaxies (Shapley et al. 2006). In contrast, Vanzella et al. (2010) found evidence for escaping Lyman continuum in only 1 of 100 Lyman Break galaxies at $z \sim 4$.

Why do only a minority of the high-z galaxies and none of the low-z galaxies show a significant leakage of ionizing radiation? In this regard, it is instructive to note that an H I column density of only 1.6×10^{17} cm^{-2} is required to produce unit optical depth at the Lyman edge. The area-averaged column densities of cold gas in star-forming galaxies are much larger, ranging from 10^{21} cm^{-2} in ordinary low-redshift galactic disks to as high as 10^{24} cm^{-2} in local starbursts and high-z star-forming galaxies (Kennicutt 1998; Genzel et al. 2010). The escape of ionizing radiation must then be determined by the topology of the interstellar medium (ISM), which will in turn

be strongly influenced by feedback from massive stars. It may be that rather exceptional circumstances are required to produce the required channels of very low column-density neutral gas. Such processes have been extensively studied from a theoretical perspective over the past decade (e.g., Dove et al. 2000; Clarke & Oey 2002; Fujita et al. 2003; Gnedin et al. 2008; Wise & Cen 2009; Razoumov & Somer-Larson 2010). These considerations provide the motivation of the present paper: to find local examples of galaxies in which a potentially significant fraction of the ionizing radiation may be escaping, and to then exploit the relative ease of observing such bright local objects to gain insight into the physical processes that facilitate this escape. To be able to assess the cosmological implications of the results of such an approach, it is important to observe local galaxies that most closely resemble the type of UV-bright high-redshift galaxies that are candidates for the reionization of the universe.

We began such an investigation in Overzier et al. (2009, hereafter O09), where we reported on *Spitzer* photometry, *Hubble Space Telescope* (*HST*) imaging, and Sloan Digital Sky Survey (SDSS) optical spectroscopy of a sample of 31 Lyman Break Analogs (LBAs). These LBAs are a very rare population of local galaxies that strongly resemble the high-z Lyman Break galaxies (Heckman et al. 2005; Hoopes et al. 2007; Overzier at al. 2008, 2010; Basu-Zych et al. 2007, 2009). They are defined to have a range in far-UV luminosity ($>2\times10^{10}\,L_{\odot}$) and far-UV effective surface brightness ($>10^{9}\,L_{\odot}$ kpc^{-2}) that are similar to typical Lyman Break galaxies.

We showed in O09 that the morphologies of LBAs as revealed in multi-band *HST* images fall into two distinct categories. The first class (25 objects) consists of galaxies in which multiple bright complexes of clumps and knots reside in a galaxy whose disturbed morphology is suggestive of a major merger or strong tidal interaction. The second class (six objects) consists of galaxies whose UV image is dominated by a single extremely massive ($M_{*}\sim$ one-to-several billion $M_{\odot}$) and compact (radius of order 100 pc) central object (a dominant central object, or DCO). We pointed out that the star formation rates derived for these six galaxies based on the extinction-corrected Hα luminosities were systematically smaller than those derived from the *Spitzer* mid-IR luminosity (by factors of ∼2–5), and speculated that a possible explanation was that these galaxies were leaking ionizing radiation into the intergalactic medium.

In this paper, we test this idea using new *HST* far-UV observations with the Cosmic Origins Spectrograph (COS) of a sample of eight LBAs from O09. We will combine these new data with archival *Far-Ultraviolet Spectroscopic Explorer* (*FUSE*) data for 3 other LBAs and for 15 more typical UV-bright local starbursts. We will describe the sample selection in Section 2 and the observations and data analysis in Section 3. We will present our results and consider their interpretation in Section 4, and summarize these results and their implications in Section 5.

2. SAMPLE SELECTION

We have previously used the Hopkins Ultraviolet Telescope and *FUSE* to search for the direct evidence of the escape of ionizing radiation from local starbursts (Leitherer et al. 1995; H01; G09), but the modest sensitivity of these facilities was sufficient only to observe three LBAs (none of which contained a DCO). With the recent installation of the COS on the *HST*, we are now in a position to obtain high-quality far-UV spectra of a significantly larger sample of these galaxies, including some with DCOs.

For the redshifts of the LBAs in our *HST* program ($z\sim$ 0.1–0.25), the sensitivity of COS is poor in the rest-frame Lyman continuum. The sensitivity is much better at longer wavelengths, so in this paper we follow H01 and G09 and use the residual intensity in the core of the strongest far-UV interstellar absorption lines from the neutral phase of the ISM as a probe of the intensity in the region below the Lyman edge. We will describe this in more detail in Section 3.

This approach requires the observations to be obtained through an aperture that encloses the bulk of the starburst's emission (so that a global constraint is obtained). It also requires that the width of instrumental spectral line-spread function is significantly smaller than the characteristic velocity dispersion in the starburst (so that the interstellar absorption lines are well resolved). Finally, the data need to have a high signal-to-noise ratio in the far-UV continuum so that useful constraints are derived.

Based on these considerations, we will consider two data sets in this paper. The first consists of the sample of 18 galaxies studied by H01 and G09. These are local starburst or star-forming galaxies observed with the *FUSE* (Moos et al. 2000), each having a signal-to-noise ratio better than 4.6 per 0.078 Å (∼25 km s^{-1}) spectral element in the *FUSE* LiF1A channel (see G09). The observations and properties of this sample are described in Table 1. Three of these galaxies are in fact LBAs without a DCO: Mrk 54 (Deharveng et al. 2001), Haro 11 (Grimes et al. 2007), and VV 114 (Grimes et al. 2006). However, most of these galaxies have considerably lower UV luminosities and star formation rates than the LBAs. They also span a much broader range in galaxy mass and metallicity (see G09 and O09, and compare Table 1 and 2).

The second is a sample of eight LBAs observed with the COS (Froning & Green 2009) on the *HST* (Program 11727: PI T. Heckman). These are members of a sample of 31 LBAs with *HST* UV images discussed by O09 and were selected for spectroscopy based on a high UV flux through the COS aperture and a compact UV size (so that the COS line-spread function is not significantly degraded). These observations and the properties of this sample are listed in Table 2 and *HST* images are shown in Figure 1. In the discussion to follow, we will refer to the eight LBAs with *HST* COS data and the three LBAs with *FUSE* data as the LBA sample. We will refer to the other 15 galaxies with *FUSE* data as the local starburst sample.

3. OBSERVATIONS AND DATA ANALYSIS

3.1. The Data

The observations and data reduction of the *FUSE* sample have been described in detail in H01 and G09. We refer the reader to these papers. All the data were obtained through the 30 × 30 arcsec LWRS aperture, except for the cases of NGC 5253 and NGC 7714 (which used the 4 × 20 arcsec MDRS aperture). As shown by G09 these apertures encompass most or all of the starburst in the far-UV. These spectra cover the observed wavelength range from 905 to 1187 Å (see Table 1 for the corresponding range in the rest frame). Depending on the angular size of the starburst in the far-UV, the instrumental spectral resolution is $R\sim$ 5000–14,000, corresponding to a velocity dispersion of $\sigma\sim$ 9 to 25 km s^{-1} (G09). In all cases, the interstellar absorption lines in the starbursts are well resolved.

For the *HST*-COS sample, we have used the COS G130M and G160M gratings to obtain spectra of our eight targets. As

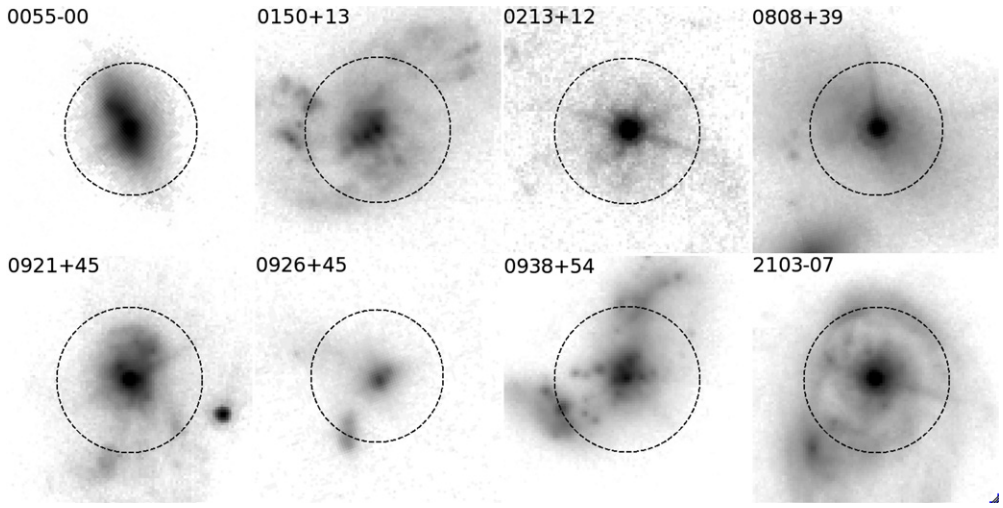

Figure 1. *HST* rest-frame optical images of the eight LBAs observed with COS. The circle indicates the 2.5 arcsec aperture of COS. For details on the images see Overzier et al. (2009). Note the diffraction spikes visible in the images of 0213+12, 0808+39, 0921+45, and 2103−07 produced by the barely resolved dominant central object.

Table 1
FUSE Sample

Name	LBA	v_{sys}	Range	$F_{esc,rel}$	$F_{esc,abs}$	SFR	log M_*	Δv_{cen}	Δv_{max}
HARO 11	Y	6175	887–1163	< 0.08	< 0.006	26	10.2	−180	−450
VV114	Y	6016	887–1164	< 0.02	<0.001	66	10.8	−150	−650
NGC 1140	N	1501	900–1181	< 0.04	< 0.014	0.83	9.4	−30	−400
SBS 0335-052	N	4043	893–1171	< 0.18	< 0.18	0.32	7.8	30	−130
TOL 0440-381	N	12291	869–1140	< 0.04	< 0.016	5.0	10.0	−120	−450
NGC 1705	N	632	903–1184	< 0.01	< 0.008	0.16	8.6	−12	···
NGC 1741	N	4037	893–1171	< 0.01	< 0.002	6.0	9.7	−35	−500
IZW 18	N	751	903–1184	< 0.1	< 0.1	0.016	7.1	−3	−150
NGC 3310	N	983	902–1183	< 0.05	< 0.005	2.8	9.8	−170	−600
HARO 3	N	963	902–1183	< 0.005	< 0.001	0.41	8.9	10	−150
NGC 3690	N	3121	896–1175	< 0.01	< 0.001	82	10.9	−120	−900
NGC 4214	N	291	904–1186	< 0.01	< 0.002	0.13	9.0	−40	−250
MRK 54	Y	13450	866–1136	< 0.09	< 0.05	21	10.4	−90	−550
M 83	N	517	903–1185	< 0.06	< 0.01	3.5	10.7	9	···
NGC 5253	N	405	904–1185	< 0.06	< 0.02	0.33	9.3	17	···
IRAS 19245-4140	N	2832	897–1176	< 0.21	<0.11	2.1	9.1	−60	−350
NGC 7673	N	3392	895–1174	< 0.1	< 0.017	4.8	10.0	−80	−350
NGC 7714	N	2803	897–1176	< 0.03	< 0.01	6.9	10.2	−60	−500

Notes. Column 1: galaxy name. Column 2: is the galaxy an LBA? See O09 for a definition. Column 3: galaxy systemic velocity (km s^{-1}) from G09 or H01. Column 4: wavelength range covered by the *FUSE* data in the galaxy rest frame (Å). Column 5: the relative escape fraction of ionizing radiation based on the residual relative intensity in the C II λ1036.3 line—see the text for details. Column 6: the absolute escape fraction including the effect of attenuation due to dust opacity—see the text for details. Column 7: the star formation rate ($M_\odot$ yr^{-1}), based on the sum of the total IR and far-UV luminosities and assuming a Chabrier (2003) IMF—see G09 for details. Column 8: the log of the galaxy stellar mass ($M_\odot$) based on the Two Micron All Sky Survey *K*-band luminosity and assuming a *K*-band mass-to-light ratio of 0.4 (Bell & de Jong 2001). Column 9: the centroid velocity of the strong interstellar absorption lines with respect to the galaxy systemic velocity (km s^{-1}). See G09 for details. Column 10: the maximum outflow velocity (in km s^{-1}), following Steidel et al. (2010).

can be seen in Figure 1, the COS aperture encompasses most or all of the galaxy. We have retrieved these data from the *HST* MAST archive after they have been processed through the standard COS pipeline. The merged spectra cover a range from about 1160 to 1780 Å with the corresponding range in the rest-frame wavelength given for each sample member in Table 2. As with the *FUSE* data, the instrumental spectral resolution depends on the angular size of the far-UV continuum within the COS aperture. Our *HST* UV images (O09) yield sizes of 0.1–0.5 arcsec (FWHM), and we estimate that the resulting spectral resolution is $R \sim 3000$–13,000, corresponding to a velocity dispersion of $\sigma \sim 10$–43 km s^{-1} (similar to the *FUSE* data).

For the new COS spectra, we have fit each merged G130M and G160M spectrum with a Starburst99 (Leitherer et al. 1999) model spectrum for a young stellar population with a metallicity similar to that of the corresponding LBA (Table 2). We did not attempt to obtain a rigorous best fit, but simply adopted a standard Chabrier (2003) initial mass function (IMF) and assumed a constant rate of star formation. We varied the duration of the star formation until we obtained (by eye) a satisfactory fit to the strong stellar wind features. We then took the ratio of the model and the data and fit the result with a low-order polynomial (avoiding spectral regions with strong emission or absorption features). We then divided the data by the polynomial

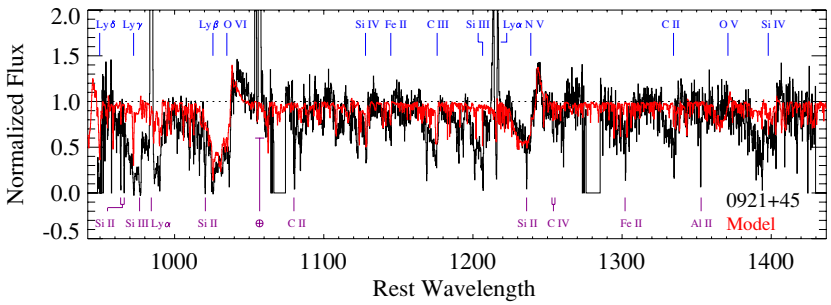

Figure 2. Full COS G130M and G160M spectrum of LBA0921+45 is shown in black, while an illustrative Starburst99 model spectrum is shown in red (constant star formation for 10 Myr with 0.4 solar metallicity and a Chabrier IMF). Both spectra have been normalized to unit flux (see the text). Prominent spectral features in the starburst are labeled at the top, while Milky Way and geocoronal features are labeled at the bottom.

Table 2
COS Sample

Name	DCO	z_{sys}	Range	$F_{esc,rel}$	$F_{esc,abs}$	SFR_{IR+UV}	$SFR_{H\alpha}$	log M_*	Δv_{cen}	Δv_{max}	R_{eqw}	β	[O/H]
0055−00	N	0.16744	970–1513	<0.05	<0.01	29	23	9.7	−230	−640	−0.21	−1.5	−0.41
150+13	N	0.14668	1022–1572	<0.1	<0.01	56	19	10.3	−150	−480	−0.78	−1.6	−0.30
0213+12	Y	0.21902	945–1440	0.35	0.05	55	6.7	10.5	−770	−1500	0.36	−0.9	0.05
0808+39	Y	0.09123	1038–1607	0.3	0.12	11	3.7	9.8	−680	−1500	0.27	−1.0	0.05
0921+45	Y	0.23499	948–1430	0.3	0.04	84	26	10.8	−650	−1500	0.75	−1.4	−0.02
0926+45	N	0.18072	968–1515	0.6:	0.4:	10	13	9.1	−300	−700	0.14	−2.3	−0.60
0938+54	N	0.10208	1029–1614	<0.1	<0.05	13	13	9.4	−90	−610	−0.17	−2.1	−0.50
2103−07	Y	0.13689	1030–1585	<0.05	<0.01	63	41	10.9	−720	−1500	0.04	−0.5	0.01

Notes. Column 1: galaxy name. Column 2: does the galaxy contain a dominant central object (DCO)? See O09 for details. Column 3: the galaxy redshift from Overzier et al. (2011). Column 4: the wavelength range covered by the COS data in the galaxy rest frame (Å). Column 5: the relative escape fraction of ionizing radiation based on the residual relative intensity in the C II λ1334.5 line. In the case of 0926+45 the C II line has a significant residual intensity, but there is no deficiency of Hα emission (unlike the cases of 0213+12, 0808+39, and 0921+45). Only these three latter objects are good candidates for the escape of ionizing radiation. See the text for details. Column 6: the absolute escape fraction including the effect of attenuation due to dust opacity—see the text for details. Column 7: the star formation rate ($M_\odot$ yr^{-1}), based on the sum of the total IR and far-UV violet luminosities and assuming a Chabrier 2003 IMF—see Overzier et al. (2011) for details. Column 8: the star formation rate ($M_\odot$ yr^{-1}), based on the extinction-corrected Hα luminosity measured from the SDSS spectra—see Overzier et al. (2011) for details. Column 9: the log of the galaxy stellar mass ($M_\odot$). See O09 for details. Column 10: the centroid velocity of the Si III λ1206.5 interstellar absorption-line with respect to the galaxy systemic velocity (km s^{-1}). Column 11: the maximum outflow velocity seen in the Si III λ1206.5 line (in km s^{-1}), following Steidel et al. (2010). Column 12: the ratio of the equivalent widths of the blueshifted and redshifted components of the Lyα line. Values near one imply significant blueshifted Lyα emission. See the text for details. Column 13: the spectral slope of the UV continuum defined by $F_\lambda \propto \lambda^\beta$. An unreddened starburst will have $\beta \sim -2.5$ to -2. Six of the eight LBAs suffer significant dust reddening. Column 14: the log of gas-phase O/H ratio relative to solar (Asplund et al. 2009). See Overzier et al. (2009) for details.

to obtain a normalized spectrum. An example of this is shown in Figure 2.

3.2. The Analysis Approach

The opacity of the ISM to Lyman continuum photons is due to two primary sources: the photoelectric opacity of the neutral hydrogen and the opacity of dust. The latter significantly affects the entire UV continuum in typical local starbursts and high-z galaxies. We will focus first on measuring constraints on the photoelectric opacity. Later we will comment on the importance of dust.

The only direct probe of the photoelectric opacity is the direct measurement of the relative intensity in the continuum shortward of the Lyman edge. The *FUSE* data provide clean access to this spectral region and adequate signal-to-noise ratio in only five targets. G09 have used these data to derive upper limits to the escape of ionizing radiation for these galaxies (see also Deharveng et al. 2001; Bergvall et al. 2006). The COS data do not sample this spectral region in any galaxy. Thus, to gain insight into the escape of ionizing radiation for our two samples we will follow H01 and G09 and use as probes the residual intensity in the core of the strongest interstellar absorption lines that primarily arise in the neutral ISM.

For the *FUSE* data, the strongest such line is C II λ1036.3 and for the *HST*-COS data the strongest such line is C II λ1334.5. Thus, in both samples we will use the same ionic species as a tracer of the neutral ISM.[9] We have measured the relative residual intensity in the core of the C II absorption line, following the same methodology as in H01 and G09. The results are listed in Tables 1 (*FUSE*) and 2 (COS).

4. RESULTS AND INTERPRETATION

4.1. The Ionization Source

Before considering constraints on the escape of ionizing radiation, it is important to establish that an ionizing population of massive stars (O stars) is in fact present in our targets. The strongest spectroscopic signature of these stars is provided by the broad P-Cygni profiles in the resonance transitions of highly ionized species that arise in the stellar winds (e.g., Robert et al. 1993, 2003).

The strongest such feature that is present in all our COS spectra is N V λ1240. In Figure 3, we show the NV profile for our

[9] In principle, a significant fraction of the gas-phase carbon in the neutral medium could be in the form of C I (which has an ionization potential of 11.52 eV). The C I λ1277.2 line should be comparable in strength to the two C II lines in this case; however, it is extremely weak in our COS spectra and in the spectra of other local starburst galaxies (e.g., Heckman et al. 1998; Leitherer et al. 2002; Schwartz et al. 2006; Leitherer et al. 2011) and high-z Lyman Break galaxies (Shapley et al. 2003; Pettini et al. 2002; Steidel et al. 2010; Quider et al. 2009, 2010; Dessauges-Zavadsky et al. 2010).

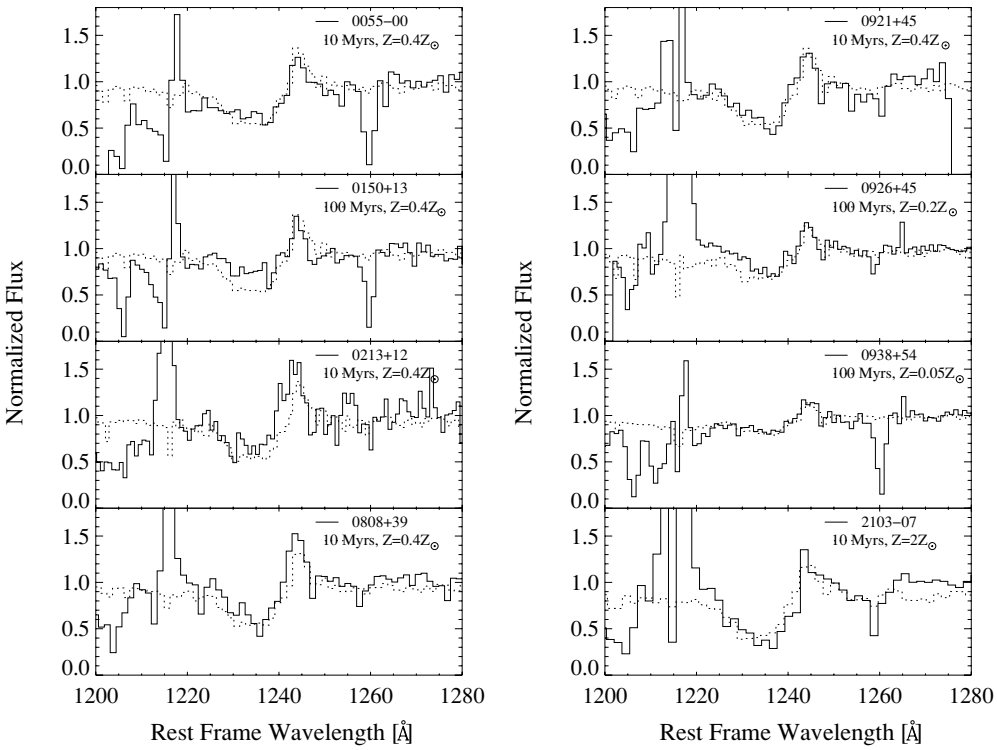

Figure 3. Spectra of the N v λ1240 stellar wind line in the eight LBAs. The dotted lines are illustrative models from Starburst99 that show that these spectra are consistent with the presence of a significant population of ionizing (O) stars. The models assume a rate of constant star formation for either 10 or 100 Myr (as indicated), a Chabrier IMF, and a metallicity as indicated.

eight targets and overplot the generic examples of Starburst99 model spectra described above. We defer to a future paper a detailed discussion of the properties of the stellar populations in the LBAs. Here, we merely point out that the far-UV spectra of the LBAs are all consistent with a normal population of ionizing stars expected for a strong starburst.

4.2. Constraints on the Escape of Ionizing Radiation

In Figure 4, we show the C II λ1334.5 absorption-line profiles for our COS data on eight LBAs. The corresponding profiles for the C II λ1036.3 line from the *FUSE* data can be found in H01 and G09. A striking result is that there is a significant residual intensity in the absorption-line profiles in four LBAs (LBA0213+12, LBA0808+39, LBA0921+45, and LBA0926+45). The first three objects all contain a DCO. These results contrast strongly with the results in H01 and G09 in which the C II λ1036.3 absorption line in the *FUSE* data is black or nearly black at line center in all cases.

To understand our approach in using the C II line as a probe of the Lyman continuum, let us consider two limiting idealized cases. In the first, we assume a picket-fence model in which the far-UV source is surrounded by a population of clouds that are optically thick in both the absorption line and the Lyman continuum and that cover a fraction f_c of the sky as seen by the source. In this case, the residual relative intensity at the core of the line (I_0) is just $I_0/I_{\rm cont} = 1 - f_c$. Thus, a significant residual intensity in the line core implies a significant escape of Lyman continuum radiation.

In the second case, we assume that the far-UV source is surrounded by a uniform shell with unit covering factor. As discussed in H01, in this case the optical depth in the ISM just below the Lyman edge is related to the optical depth at the core of the absorption line by

$$\tau_{\rm Ly}/\tau_0 = R Z_{\rm gas}^{-1} (\sigma_{\rm gas}/100\,{\rm km\,s^{-1}}), \quad (1)$$

where $Z_{\rm gas}$ is the gas-phase carbon abundance scaled to the solar value of log(C/H) + 12 = 8.43 (Asplund et al. 2009), we assume that C II is the dominant ionization state in the neutral gas, $\sigma_{\rm gas}$ is the velocity dispersion in the neutral gas, and R = 17 and 12 for the 1036.3 and 1334.5 lines, respectively (Morton 2003). Since the optical depth at the Lyman edge is over an order of magnitude larger than in the line core, in this idealized case a significant residual intensity in the core of the absorption lines is a necessary but not sufficient condition for the escape of ionizing radiation.

To test these two models, we have used the set of Si II absorption lines available in the COS data. Like C II, Si II is the dominant ion of silicon in the neutral ISM. By using lines that all arise in the same ionic species, but which span a range in oscillator strengths, a comparison of the absorption profiles among these lines allows us to estimate the optical depth and covering factor of the gas (e.g., Heckman et al. 2000; Rupke et al. 2002; Quider et al. 2009; Erb et al. 2010). In the case of optically thick clouds that do not fully cover the far-UV source, the line profiles of the different transitions should look the same. In the case of a uniform shell, the residual intensity will increase with decreasing oscillator strength f (since $\tau_0 \propto \lambda f$). We will use the following transitions (with the respective values of log λf from Morton 2003): Si II λ1260.4 (−1.32), 1193.3 (−1.65), and 1190.4 (−1.95).[10]

[10] Unfortunately, the Si II 1526 line (−2.18) is accessed in only one object and the 1304.4 line (−2.44) is badly blended with the Si III λ1301.2,1303.3 stellar photospheric features (Walborn et al. 1995; Massa 1989) and the adjacent O I λ1302.2 interstellar line.

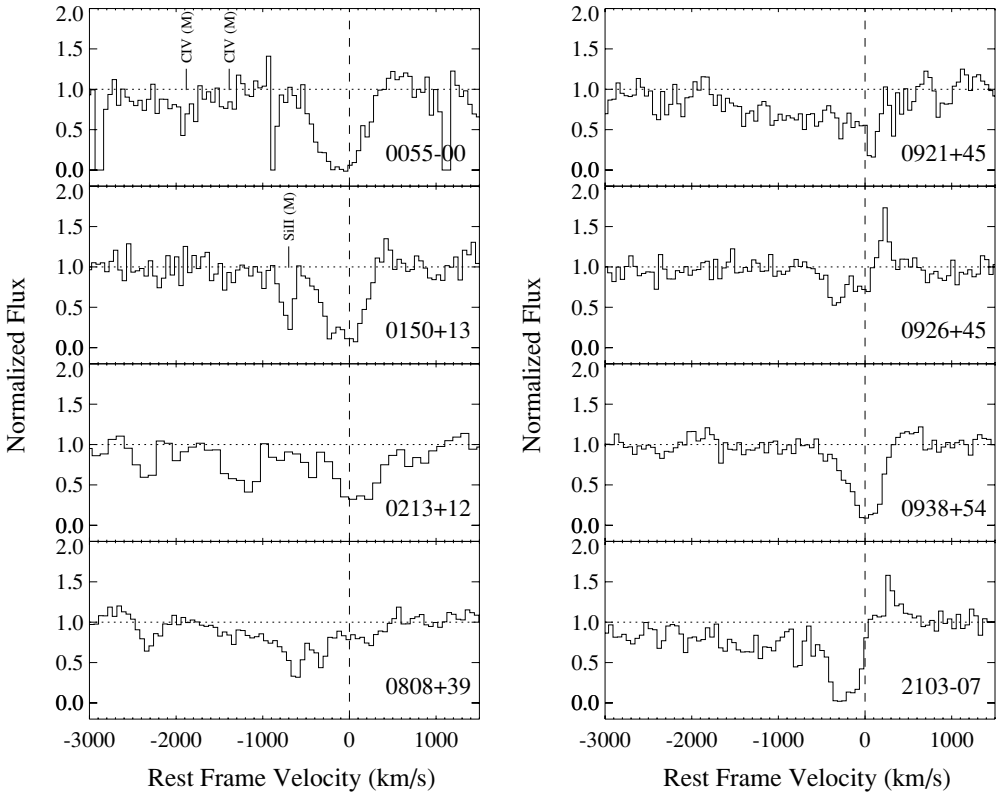

Figure 4. Absorption-line profiles of the C II λ1334.5 feature. The dotted line indicates the galaxy systemic velocity derived from SDSS spectra. Contaminating foreground Milky Way features are noted. There is a significant relative residual intensity in the line profile in four cases (0213+12, 0808+39, 0921+45, and 0926+45).

For each galaxy, we simultaneously fit a single Gaussian profile to the three different Si II lines, forcing the three lines to share a common centroid and width but allowing the normalization (depth) of each line to vary freely. In all four galaxies, the results strongly favor the picket-fence model with an implied covering factor of optically thick clouds of about 40% for LBA0213+12 and LBA0926+45, 50% for LBA0808+39, and 60% for LBA0921+45. We show these fits for the case of LBA0921+45 in Figure 5.[11] In principle, the sightlines that avoid the clouds could be optically thin to the metal lines but still be optically thick to the Lyman continuum (Equation (1)). Thus, confirmation that there is significant escaping ionizing radiation will require direct observations below the Lyman edge in these cases.

In the meantime, we can consider whether there is other evidence for the escape of ionizing radiation in these four LBAs. In O09, we highlighted the relative weakness of the extinction-corrected Hα emission line in most of the LBAs with DCOs, and speculated that a significant fraction of the ionizing radiation might be escaping. This information is listed in Table 2 where we compare the star formation rates derived from the extinction-corrected Hα emission line ($SFR_{H\alpha}$) to that obtained from the sum of the total IR and far-UV luminosity (SFR_{IRUV}). It is noteworthy that three of the four objects above in which we have inferred an incomplete covering of the far-UV source by neutral clouds have the highest ratios of $SFR_{IRUV}/SFR_{H\alpha}$: LBA0213+12 (a ratio of 8.2), LBA0808+39 (3.0), and LBA0921+45 (3.2). All three of these contain a DCO. In contrast, the mean ratio of $SFR_{IRUV}/SFR_{H\alpha}$ for the other five galaxies is 1.4. Thus, based on two independent lines of evidence, we suggest that there is a significant leakage of ionizing radiation from three of the eight LBAs in our sample.

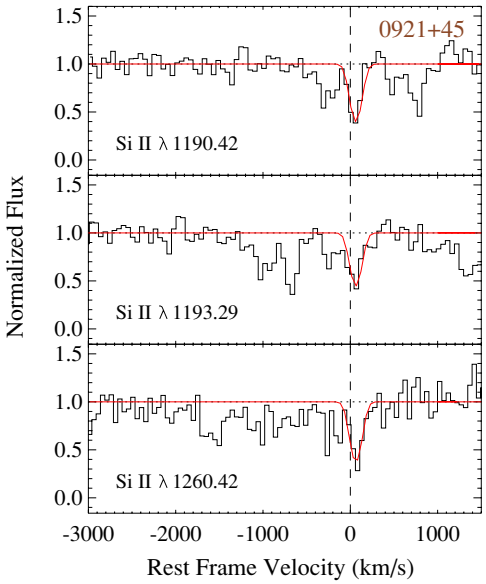

Figure 5. All Si II 1190.4, 1193.3, and 1260.4 absorption-line profiles for LBA0921+45 plotted on the same scale. In each panel, the red line shows a fit of a single Gaussian to the strongest component of the profile. This was a joint simultaneous fit to all three features, which were forced to have a common centroid and line width, but a free line depth. The similar fitted depth of the feature in all three cases shows that the data imply gas that is optically thick, but does not fully cover the continuum source (a picket-fence model). See the text for details.

How do these results compare to what is seen at high redshift? There are four gravitationally lensed high-z galaxies that have

[11] For the other four LBAs, the data imply that the Si II lines are optically thick but fully cover the far-UV continuum source.

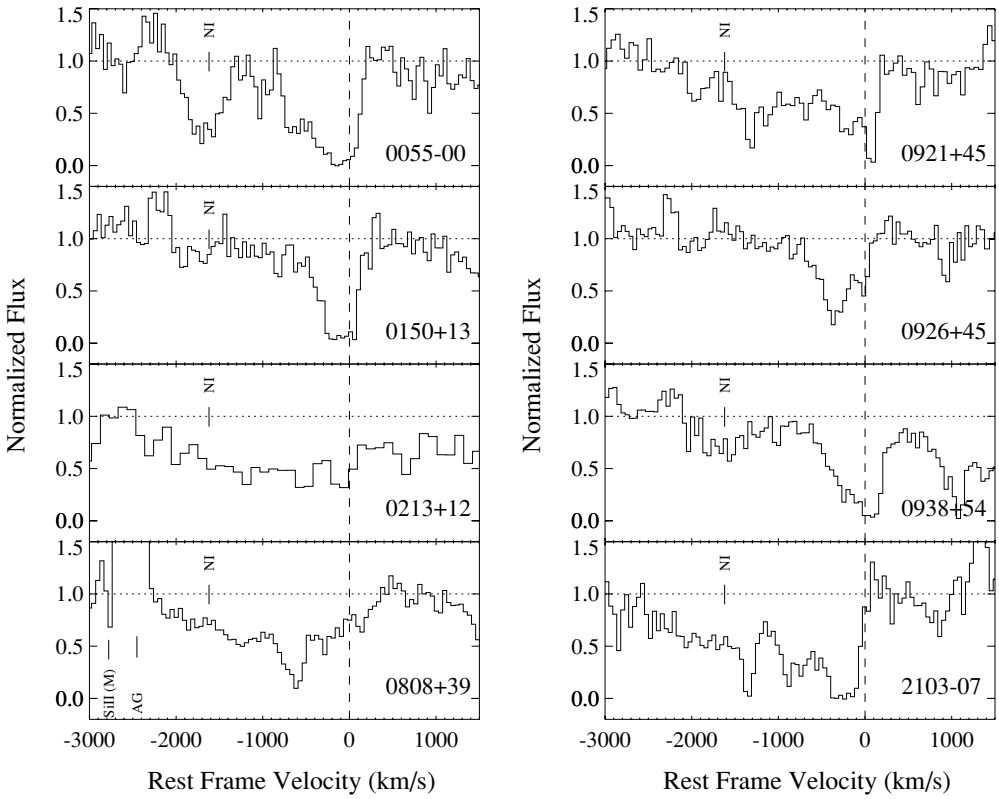

Figure 6. Absorption-line profiles of the Si III λ1206.5 feature. Contaminating foreground Milky Way and air-glow features are noted. Highly blueshifted absorbing material is detected up to at least −1500 km s^{-1} in the four cases with a dominant central object (see the text). Beyond this velocity, there is possible contamination by the N I λ1200.0 feature (as marked).

been observed with spectral resolution and signal-to-noise ratio similar to our sample.[12] Of these, the residual relative intensities of C II λ1334.5, O I λ1302.2, and Si II λ1260.4 (the strongest metal lines tracing the neutral ISM) are very small in MS 1512-cB58 (Pettini et al. 2002), The Cosmic Eye (Quider et al. 2010), and the 8 O'Clock Arc (Dessauges-Zavadsky et al. 2010), but large (∼40%) in The Cosmic Horseshoe (Quider et al. 2009). In fact, the last object appears to a good example of the type of picket-fence situation seen in the DCOs in our sample.

As discussed above, dust can also be a significant source of opacity to ionizing radiation in galaxies. Following Shapley et al. (2006) and G09, we can distinguish between the absolute and relative escape fractions. The former is the actual fraction of ionizing photons that escape the galaxy, including the effect of dust. The latter neglects the effect of dust and is defined as the ratio of the fraction of escaping ionizing photons to escaping non-ionizing far-UV photons (e.g., it measures only the effect of the photoelectric opacity of the gas). Our measurements discussed above provide information about the relative escape fraction. Given that the ratio of far-IR to far-UV fluxes for the galaxies with DCOs are of order 10, the implied absolute escape fractions will be proportionately smaller. We list our estimates for both the relative and absolute escape fractions in Tables 1 (*FUSE*) and 2 (COS).

[12] These strong interstellar metal absorption lines from neutral gas exhibit significant residual intensity in the high signal-to-noise ratio stacked spectra of high-z star-forming galaxies (e.g., Shapley et al. 2003; Steidel et al. 2010). However, these data are obtained at relatively low spectral resolution ($R \sim 10^3$), so that the line profiles are not well resolved in individual objects (and could miss gas with a high covering factor but low velocity dispersion). The stacking process itself could also smear out black, narrow components found in the spectra of individual galaxies.

4.3. Extreme Feedback

As can be seen in Figure 4, the C II λ1334.5 absorption-line profiles in all the LBAs are blueshifted with respect to the galaxy systemic velocity, implying a large-scale outflow of gas. Further evidence for outflows is provided by the broad blue-asymmetric wings seen on the optical emission-line profiles (O09).

The absorption-line profiles in Figure 4 show evidence for exceptionally high outflow speeds in the DCOs. To further investigate this, we turn to the Si III λ1206.5 feature. This is the strongest metal line that is accessed in all four DCO spectra, and arises in the ionized gas. As shown in Figure 6, outflowing gas is detected at extraordinarily high velocities in all four galaxies with DCOs. The flux-weighted line centroid is blueshifted by about 700 km s^{-1} in these objects (Table 2). It is difficult to determine the maximum outflow velocity because of blending with the N I λ1200 triplet, which lies ∼1600 km s^{-1} blueward of the Si III line. Conservatively, the maximum outflow speed seen in the DCOs reaches at least 1500 km s^{-1}.

These velocities are much higher than in the local starburst sample and in the LBAs without a DCO. This is shown in Figure 7 where we plot the outflow speeds in the ionized gas in local starburst and LBA samples versus the star formation rate and galaxy mass (see Tables 1 and 2). For galaxies with *FUSE* data, we use the C III λ977.0 and/or N II λ1084.0 and/or C II λ1036.3 lines.

The outflow velocities in the DCOs are also significantly larger than those typically seen in high-z galaxies. Steidel et al. (2010) find line centroids that are blueshifted on-average by 164 km s^{-1} and maximum outflow speeds that are typically ∼800 km s^{-1} for galaxies with star formation rates of $\sim 10^1$–$10^2 M_\odot$ yr^{-1}.

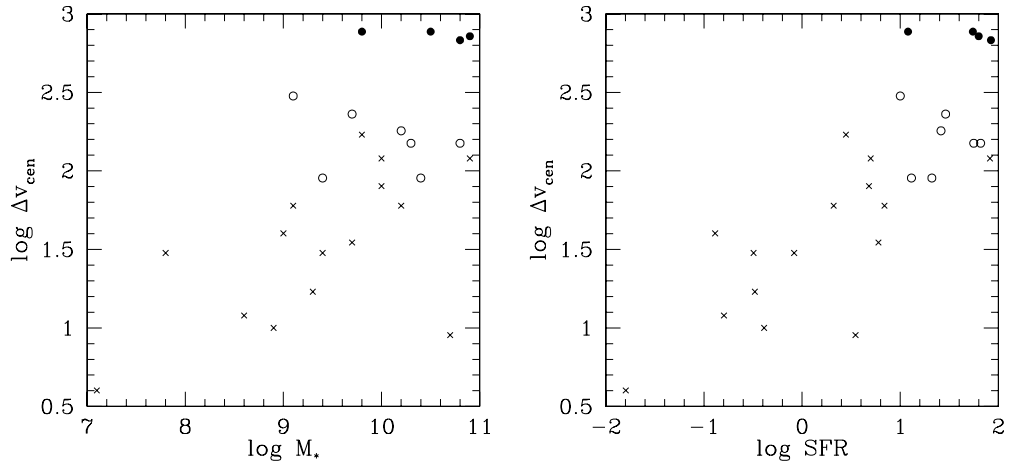

Figure 7. Plots of the outflow velocity (km s^{-1}) defined by the line centroid as a function of the galaxy stellar mass ($M_\odot$) and the star formation rate ($M_\odot$ yr^{-1}). The typical local stabursts are indicated by crosses and the LBAs with and without dominant central objects are indicated by solid and hollow dots, respectively. The exceptionally high outflow speeds associated with the dominant central objects are clear. See Tables 1 and 2.

Outflows from intensely star-forming galaxies are believed to be produced as gas clouds are accelerated by the ram pressure of a hot and fast wind driven by the collective thermal/kinetic energy supplied by supernovae and massive stellar winds (e.g., Heckman et al. 2000; Veilleux et al. 2005; Marcolini et al. 2005), and/or by radiation pressure acting on dust (Murray et al. 2005, 2010). Can the unusually high velocities seen in the DCOs be explained in this way? We consider a simple idealized model of a cloud with a column density N accelerated outward from an initial radius r_0 by the ram pressure of a wind that carries momentum at a rate $\dot{p}$ into a solid angle Ω. Then, the terminal velocity of this cloud will be

$$v_{\rm term} = 1800 \dot{p}_{35}^{1/2} (\Omega/4\pi)^{-1/2} r_{0,100}^{-1/2} N_{21}^{-1/2} \,{\rm km\,s^{-1}}. \quad (2)$$

Here, the momentum flux is in units of 10^{35} dynes, the initial radius is in units of 100 pc and the cloud column density is in units of 10^{21} cm^{-2}. The DCO star formation rates imply momentum fluxes of this order (Leitherer & Heckman 1995), while the *HST* images yield typical DCO radii of 100 pc (O9). As discussed below in Section 4.6, a column density of 10^{21} cm^{-2} is a reasonable estimate for the ionized gas in these objects.

The above neglects gravitational forces (cf. Wang 1995; Martin 2005; Murray et al. 2010). This is justified here because the typical sizes and radii of the DCOs imply virial velocities of only about 200 km s^{-1} (much smaller than the maximal outflow speeds we observe). Note that Murray et al. (2010) conclude that outflows driven out of massive star clusters by radiation pressure will only have outflow speeds of order the local escape velocity. This is not the case in the DCOs.

These considerations imply that a galactic wind driven by an extreme starburst can in principle accelerate clouds to the high velocities that we see in the DCOs. The significantly higher velocities in these galaxies compared to typical starbursts can be naturally explained by the combination of a large number of massive stars confined within an unusually small radius. This leads to a very large wind ram pressure and/or radiation pressure at the launch point of the clouds.

4.4. Feedback from an Active Galactic Nucleus?

An alternative form of extreme feedback could be provided by an AGN. As discussed in Overzier et al. (2009), the optical spectra of the LBAs with DCOs may imply a composite of both an intense starburst and an obscured (Type 2) AGN. The COS data show that the far-UV radiation in these objects is dominated by light produced by hot massive stars (Figures 2 and 3), which does not rule out the presence of a Type 2 AGN.

Recent observations with *XMM-Newton* (Jia et al. 2010) show that LBAs with such apparently composite optical spectra are also over-luminous in the 2–10 keV X-ray band by the factors of roughly 3–30 compared to pure starbursts of the same far-IR luminosity. They conclude that it is likely that at least some of these objects do harbor an AGN, but that the overall bolometric luminosity of the galaxy is primarily due to an intense starburst. Could a Type 2 AGN be responsible for the unusually high outflow speeds and/or the apparently low covering factor of neutral gas due to a highly ionized state of the ISM?

Very high outflow speeds (many thousands of km s^{-1}) are commonly observed in *unobscured* (Type 1) AGN (e.g., Rupke et al. 2005; Krug et al. 2010). However these same authors show that outflows similar to those we see in the DCOs (maximum outflow speeds of at least 1500 km s^{-1}) are extremely rare in composite obscured-AGN/starburst systems and not seen at all in "pure" obscured AGN. They conclude that the AGN can drive very high-speed outflows, but these flows are confined to a small region very near the black hole (and are hence undetectable in Type 2 AGN). They also conclude that the AGN plays little or no role in driving the large-scale outflows seen in the composite systems. It therefore seems unlikely that the high velocity outflows in the DCOs are driven by an obscured AGN.

Tremonti et al. (2007) have detected outflows at velocities ranging from 500 to 2000 km s^{-1} in massive post-starburst galaxies at $z \sim 0.6$. They speculate that such high velocities may require an AGN-driven outflow. It is also possible that these objects are more massive versions of the DCOs in this paper. This could be confirmed by *HST* imaging of their galaxies.

4.5. Clues from Lyα

The properties of the Lyα profile are highly sensitive to the kinematics and distribution of the outflowing gas and dust in star-forming galaxies (e.g., Steidel et al. 2010; Hansen & Oh 2006; Verhamme et al. 2006, 2008; Kornei et al. 2010). In Figure 8, we plot the Lyα profiles for the eight LBAs with COS data, and highlight one very suggestive trend.

In the five cases in which the inferred relative escape fraction is small, there is very little (if any) Lyα emission blueward of

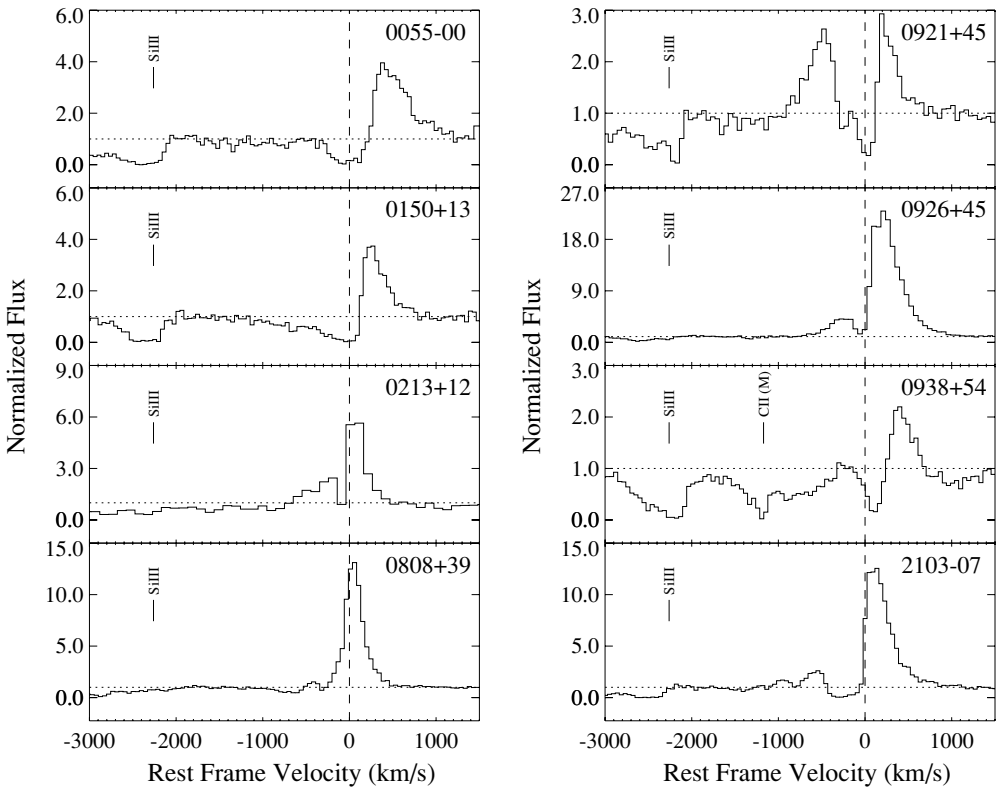

Figure 8. Plots of the Lyα feature. The location of the Si III λ1206.5 feature is noted, as are the locations of foreground Milky Way features. In three cases (0213+12, 0808+39, and 0921+45), there is a significant amount of blueshifted Lyα emission. These are the three objects that are candidates for a significant escape fraction of ionizing radiation.

the systemic velocity. Instead, the profiles show Lyα emission redward of the systemic velocity and either pure absorption or a mix of absorption and weak emission to the blue. Such profiles are typical of high-z star-forming galaxies (e.g., Shapley et al. 2003; Steidel et al. 2010). In contrast, for the three objects in which we infer a high relative escape fraction (LBA0213+12, 0808+39, and 0921+45) a significant fraction of the Lyα emission is blueshifted with respect to the systemic velocity. To quantify this, we have measured the net equivalent widths (emission − absorption) blueward and redward of the systemic velocity in these eight LBAs. We define net emission (absorption) to have a positive (negative) equivalent width. We then take the ratio of the red and blue equivalent widths ($R_{\rm eqw}$).

We list the results in Table 2. For the five galaxies with low inferred escape fractions $R_{\rm eqw}$ is either negative (redshifted emission and blueshifted absorption) or small and positive (strong redshifted emission and weak blueshifted net emission): LBA0055−00 ($R_{\rm eqw} = -0.21$), 0150+13 (−0.78), 0926+45 (0.14), 0938+54 (−0.17), and 2103−07 (0.04). For the three galaxies with high inferred escape fractions $R_{\rm eqw}$ is of order one and positive (similar amounts of redshifted and blueshifted emission): 0213+12 ($R_{\rm eqw} = 0.36$), 0808+39 (0.27), and 0921+45 (0.75).

Profiles with significant blueshifted emission are uncommon but not unknown in star-forming galaxies at $z \sim 2$–3. Verhamme et al. (2008) discuss two such cases and interpret them as arising due to radiative transfer effects in a static medium. This model cannot be correct for the three DCOs in Figure 8 because the metal lines demonstrate that the gas is rapidly outflowing (Figures 4 and 6). Erb et al. (2010) discuss the case of a high-z galaxy with both an outflow detected in the metal lines and a significant amount of blueshifted Lyα emission. They argue that in this case the optical depth to Lyα photons is unusually low in the foreground outflowing material and that this is naturally related to the low covering factor of neutral gas they infer in this object (precisely the situation we see in our three galaxies).

4.6. Where is the Dust?

It is important to note that the observed UV spectral energy distributions (SEDs) of the DCOs are significantly redder than the intrinsic SED of a starburst (Overzier et al. 2011, and see Table 2). For a normal starburst or Small Magellanic Cloud (SMC) dust attenuation law (Calzetti 2001; Leitherer et al. 2002), these SEDs imply roughly two magnitudes of dust extinction along the line of sight to the DCO in the far-UV. This then raises a very interesting question. How can there be this much dust when the observations of interstellar absorption lines from the neutral gas imply that such gas only covers a fraction of the far-UV source? The answer must be that this dust is associated with *ionized* gas that covers most or all of the DCO.

This picture requires that the cores of the strongest absorption lines due to the ionized gas should be nearly black (unlike the case of lines from the neutral phase). Examination of the profiles in Figure 6 shows that this is the case in LBA0808+39 (a relative residual intensity in the Si III λ1206.5 line of 10%), LBA0921+45 (7%), and LBA2103−07 (<3%). In the case of LBA0213+12, the relative residual intensity in this line is high (∼40%). However, the redshift of this galaxy is large enough to shift the C III λ977.0 line into the COS G130L spectrum. This should be the strongest interstellar line due to ionized gas, and as such provides the most sensitive probe. Although the data are noisy, the relative residual intensity in this line is small (10% or

less). Thus, in this galaxy the Si III line is optically thin, while the C III line is optically thick.

We therefore conclude that the ionized gas has a near-unit covering factor in the DCOs. One plausible physical model would be that the neutral gas represents the denser cores of clouds being accelerated by the wind, while the ionized gas represents a lower density halo of gas and dust surrounding the cloud core and which is being ablated by the wind and photoionized by the intense radiation field (e.g., Marcolini et al. 2005).

Can the DCO photoionize a column of gas with the required amount of dust? Elementary considerations of photoionization equilibrium imply that a source of radiation can photoionize a Stromgren slab with a column density given by

$$N_{\rm Strom} = 1.2 \times 10^{23} U \ {\rm cm}^{-2}, \quad (3)$$

where U is the dimensionless ionization parameter defined as the ratio of the density of ionizing photons to electrons in the slab. In order for a significant fraction of ionizing photons to escape, the actual gas column must be less than this value (to provide matter-bounded conditions). The optical depth due to dust in the far-UV (1500 Å) is related to the gas column density by

$$N_{\rm gas} = 3(5) \times 10^{20} \tau_{\rm FUV} Z_{\rm gas}^{-1} \ {\rm cm}^{-2}, \quad (4)$$

where the coefficients refer to an SMC (starburst) dust attenuation law (Leitherer et al. 2002) and we assume that the dust-to-gas ratio is proportional to the metallicity. The LBAs with DCOs all have gas-phase oxygen abundances close to solar (O09) and the line-of-sight reddening implies $\tau_{\rm FUV} \sim 2$. Thus, to explain the line-of-sight reddening toward the DCOs in a matter-bounded situation we need $U > 7 \times 10^{-3}$.

Alternatively, the optical depth at the Lyman edge due to neutral hydrogen in (mostly) ionized gas with a column density $N_{\rm H\,II}$ is given by

$$\tau_{\rm Ly} = 8.6 \times 10^{-24} N_{\rm H\,II} U^{-1}. \quad (5)$$

For $N_{\rm H\,II} = 10^{21}$ cm^{-2}, we require $U > 8 \times 10^{-3}$ for $\tau_{\rm Ly} < 1$.

Is this plausible? Heckman et al. (1990) and Lehnert & Heckman (1996) showed that the observed radial gas density profiles seen in the optical emission-line nebulae in starburst winds are consistent with theoretical expectations for photoionized clouds exposed to the ram pressure of the hot wind fluid (Chevalier & Clegg 1985). It is straightforward to show that in this case the ionization parameter in the clouds is given by

$$U = 9 \times 10^{-3} Q_{55} / \dot{p}_{35}, \quad (6)$$

where $\dot{p}_{35}$ is the wind momentum flux in units of 10^{35} dynes and Q_{55} is the starburst ionizing photon production rate in units of 10^{55} s^{-1}.

The ionizing photons are produced by the most massive stars with lifetimes <4 Myr, while the momentum in the starburst wind derives primarily from supernovae (whose progenitors have lifetimes of <40 Myr). In equilibrium (e.g., a constant rate of star formation for longer than 40 Myr), $Q_{55}/\dot{p}_{35} \sim 0.5$ and so $U \sim 5 \times 10^{-3}$. More generally, this ratio will be time dependent. For example, values of $U > 10^{-2}$ are associated with constant star formation for a duration less than 20 Myr and for an age <4 Myr in an instantaneous burst. These ages are consistent with current constraints on the DCOs (O09 and see Figure 3).[13]

[13] We assume a standard Chabrier (2003) IMF and use the Starburst99 models (Leitherer et al. 1999).

We therefore conclude that it is feasible for the DCOs to photoionize a matter-bounded column of gas that is sufficient to contain enough dust to produce the observed reddening and the inferred attenuation of the far-UV continuum and yet have a photoelectric opacity at the Lyman edge that is less than one.

5. SUMMARY AND IMPLICATIONS

One of the major goals in cosmology is to understand the process by which the universe was reionized. The most plausible source for the ionizing photons is an early generation of hot massive stars in forming galaxies. The primary uncertainty at present is the unknown fraction of such ionizing photons that are able to escape from the galaxies and reach the neutral hydrogen in the intergalactic medium. The column densities of gas associated with such intense star formation correspond to extremely high optical depths in the Lyman continuum. It seems nearly certain that some form of feedback from the massive stars is required to produce the pathways through which the ionizing photons can escape.

Our understanding of how this might occur would be greatly improved if we could find local examples of galaxies from which significant ionizing radiation is escaping, and could then investigate in some detail the physical processes that enable this to occur. This will be most germane to the early universe if these local galaxies are good analogs to intensely star-forming galaxies at high redshift.

Accordingly, in this paper we used the *HST* COS and the *FUSE* to investigate the far-UV properties of a sample of 11 LBAs. These rare local objects are very similar to high-z Lyman Break galaxies in all their properties studied to date (Heckman et al. 2005; Hoopes et al. 2007; Basu-Zych et al. 2007, 2009; Goncalves et al. 2010; Overzier et al. 2009, O09; Overzier et al. 2008, 2010, 2011). We have compared these rare objects to a sample of 15 typical UV-bright local starbursts.

Following Heckman et al. 2001 (H01) and Grimes et al. 2009 (G09), we have used the relative residual intensity in the cores of the strongest interstellar absorption-lines arising in the neutral ISM (the C II λ1036.5 and C II λ1334.5 lines) as a probe of the effects of the photoelectric opacity of the ISM on the Lyman continuum. This approach is made possible by the high spectral resolution ($R \sim 10^4$) and good signal-to-noise ratio in our data.

We find that there is a significant residual intensity (∼30%–50%) in the C II line core in 4 out of 11 of the LBAs but in none of the 15 typical local starbursts. We show that in all four of these cases the residual intensity reflects an incomplete covering of the far-UV source by optically thick clouds (a picket-fence model). Independent evidence for a significant escape of ionizing radiation is provided by the anomalously weak Hα emission (relative to the sum of the far-UV and far-IR emission) in three of these four galaxies. It is therefore plausible that a significant fraction of the Lyman continuum is escaping in three of the LBAs in our sample.

Assuming that the residual intensity in these lines does indicate the escape of ionizing radiation, then following Shapley et al. (2006) and G09, the relative escape fraction in these objects (defined as the ratio of fractions of escaping ionizing to non-ionizing far-UV photons) is ∼30%–40%. After accounting for the effect of dust attenuation, the absolute escape fractions are ∼3%–10%.

We have also examined the profiles of the Lyα line in the COS data of the eight LBAs for additional clues. We find that there is strong emission both blueward and redward of the systemic velocity in the three objects in which a high escape fraction is

likely. This strongly suggests an incomplete covering of the far-UV source by neutral clouds (in agreement with the properties of the metal lines). The other five cases show the profiles typically seen in high-z galaxies: Lyα emission redward of the systemic velocity and either pure absorption or a mix of absorption and weak emission blueward.

In all three cases, with high inferred relative escape fractions the *HST* images reveal that most of the far-UV emission originates in a single DCO. These are highly compact (radii $\sim 10^2$ pc) and massive (one to a few $\times 10^9 M_\odot$) young starbursts (O09). The interstellar absorption lines in all four of the LBAs with DCOs show extremely high outflow speeds: the line centroids are blueshifted by about 700 km s^{-1} and the gas reaches maximum outflow velocities of at least 1500 km s^{-1}. These are significantly higher than the velocities seen in other low redshift starbursts or in typical high-redshift galaxies. We have shown that these high speeds can be explained in principle by the acceleration of gas clouds in a starburst-driven wind. The exceptionally high velocities would be due to a large amount of momentum deposition in such an unusually small region, leading to an extremely high wind ram pressure and/or radiation pressure at the launch point for the clouds.

The far-UV emission from the DCOs is significantly reddened and attenuated by dust. We have argued that this dust must reside in the ionized gas and have shown that the ionized gas fully covers the far-UV source (the DCO). This situation is made possible by the intense ionizing radiation field in these galaxies (leading to significant column densities of dusty ionized gas that is optically thin in the Lyman continuum).

Based on the above considerations, it is tempting to link the escape of ionizing radiation to the extreme feedback associated with the DCOs. The combination of a high rate of energy deposition (kinetic energy and ionizing radiation) within such a small volume may be the key to excavating channels through the ISM and also intensely irradiating these channels so that they are fully ionized and translucent to ionizing radiation.

It is interesting that only 19% (6/31) of the sample of LBAs imaged by O09 contain a DCO. Together with the present results this would suggest that large relative escape fractions are present in only 13% of LBAs. This is similar to the fractions seen in high-redshift galaxies (Shapley et al. 2006; Iwata et al. 2009). Could the presence or absence of DCOs in these galaxies explain these results as well?

It is important to note that in the sample of LBAs studied by Overzier et al. (2009), the DCOs were preferentially found in the most massive galaxies ($M_* \sim 10^{10}$–$10^{11}\ M_\odot$). Galaxies this massive are exceedingly rare at $z > 7$, when the universe was reionized, and so the DCO host galaxies will not resemble the population of low-mass systems believed to be responsible for producing most of the ionizing radiation at these early epochs (e.g., Bouwens et al. 2010). We are instead suggesting that objects similar to the DCOs in this paper may exist in these early galaxies and facilitate the escape of ionizing radiation. A number of theoretical papers over the past decade have investigated the processes that regulate the escape of Lyman continuum radiation from galaxies (e.g., Dove et al. 2000; Clarke & Oey 2002; Fujita et al. 2003; Gnedin et al. 2008; Wise & Cen 2009; Razoumov & Somer-Larson 2010). These studies are at least qualitatively consistent with what we have observed in the DCOs.

Finally, we note that O09 have shown that the masses and sizes of the DCOs are consistent with the regions of excess mass (cusps) seen in the centers of typical present-day M_* elliptical galaxies (Hopkins et al. 2009). If so, then such galaxies may have all passed through an early stage during which they were sources of a significant amount of ionizing radiation that was able to reach the intergalactic medium.

Based on observations with the NASA/ESA *Hubble Space Telescope*, which is operated by the Association of Universities for Research in Astronomy, Inc., under NASA contract NAS 5-26555. The observations are associated with GO programs 10920, 11107, and 11727.

Facilities: HST(COS), GALEX, *Spitzer*

REFERENCES

Asplund, M., Grevasse, N., Sauval, A., & Scott, P. 2009, ARA&A, 47, 481
Basu-Zych, A., et al. 2007, ApJS, 173, 457
Basu-Zych, A., et al. 2009, ApJ, 699, L118
Bell, E., & de Jong, R. 2001, ApJ, 550, 212
Bergvall, N., Zackrisson, E., Andersson, B.-G., Arnberg, D., Masegosa, J., & Ostlin, G. 2006, A&A, 448, 513
Bouwens, R., et al. 2010, arXiv:1006.4360
Calzetti, D. 2001, PASP, 113, 1449
Chabrier, G. 2003, PASP, 115, 763
Chevalier, R., & Clegg, A. W. 1985, Nature, 317, 44
Clarke, C., & Oey, M. S. 2002, MNRAS, 337, 1299
Cowie, L. L., Barger, A. J., & Trouille, L. 2009, ApJ, 697, L122
Deharveng, J.-M., Buat, V., LeBrun, V., Milliard, B., Kunth, D., Shull, J. M., & Gry, C. 2001, A&A, 375, 805
Dessauges-Zavadsky, M., D'Odorico, S., Schaerer, D., Modigliani, A., Tapken, C., & Vernet, J. 2010, A&A, 510, 26
Dove, J., Shull, J. M., & Ferrara, A. 2000, ApJ, 531, 846
Dunkley, J., et al. 2009, ApJS, 180, 306
Erb, D., Pettini, M., Shapley, A., Steidel, C., Law, D., & Reddy, N. 2010, ApJ, 719, 1168
Fan, X., et al. 2006, AJ, 132, 117
Fernandez-Soto, A., Lanzetta, K, & Chen, H.-W. 2003, MNRAS, 342, 1215
Froning, C., & Green, J. 2009, Astrophys. Space Sci., 320, 181
Fujita, A., Martin, C., MacLow, M., & Abel, T. 2003, ApJ, 599, 50
Genzel, R., et al. 2010, MNRAS, 407, 2091
Giallongo, E., Cristiani, S., D'Odorico, S., & Fontana, A. 2002, ApJ, 568, L9
Gnedin, N., Kravtsov, A., & Chen, H.-W. 2008, ApJ, 672, 763
Goncalves, T., et al. 2010, ApJ, 724, 1373
Grimes, J., Heckman, T., Hoopes, C., Strickland, D., Aloisi, A., Meurer, G., & Ptak, A. 2006, ApJ, 648, 310
Grimes, J., et al. 2007, ApJ, 668, 891
Grimes, J., et al. 2009, ApJS, 181, 272
Hansen, M., & Oh, S.-P. 2006, MNRAS, 367, 979
Heckman, T., Armus, L., & Miley, G. 1990, ApJS, 74, 833
Heckman, T., Lehnert, M., Strickland, D., & Armus, L. 2000, ApJ, 129, 493
Heckman, T., Robert, C., Leitherer, C., Garnett, D., & van der Rydt, F. 1998, ApJ, 503, 646
Heckman, T., Sembach, K., Meurer, G., Leitherer, C., Calzetti, D., & Martin, C. L. 2001, ApJ, 558, 56
Heckman, T., et al. 2005, ApJ, 619, L35
Hoopes, C., et al. 2007, ApJS, 173, 441
Hopkins, P., Hernquist, L., Cox, T., Keres, D., & Wuyts, S. 2009, ApJ, 691, 1424
Hurwitz, M., Jelinsky, P., & Dixon, W. V. 1997, ApJ, 481, L31
Inoue, A., Iwata, I., Deharveng, J.-M., Buat, V., & Burgarella, D. 2005, A&A, 435, 471
Iwata, I., et al. 2009, ApJ, 692, 1287
Jia, J.-J., Ptak, A., Heckman, T., Overzier, R., Hornschemeier, A., & LaMassa, S. 2010, ApJ, submitted
Kennicutt, R. 1998, ApJ, 498, 541
Kornei, K., Shapley, A., Erb, D., Steidel, C., Reddy, N., Pettini, M., & Bogosavljevic, M. 2010, ApJ, 711, 693
Krug, H., Rupke, D., & Veilleux, S. 2010, ApJ, 708, 1143
Lehnert, M., & Heckman, T. 1996, ApJ, 462, 651
Leitherer, C., Ferguson, H., Heckman, T., & Lowenthal, J. 1995, ApJ, 454, L19
Leitherer, C., & Heckman, T. 1995, ApJS, 96, 9
Leitherer, C., Li, I.-H., Calzetti, D., & Heckman, T. 2002, ApJS, 104, 303
Leitherer, C., Tremonti, C., Heckman, T., & Calzetti, D. 2011, AJ, 141, 37
Leitherer, C., et al. 1999, ApJS, 123, 3
Malkan, M., Webb, W., & Konopacky, Q. 2003, ApJ, 598, 878

Marcolini, A., Strickland, D., D'Ercole, A., Heckman, T., & Hoopes, C. 2005, MNRAS, 362, 626
Martin, C. 2005, ApJ, 621, 227
Massa, D. 1989, A&A, 224, 131
Moos, H.-W., et al. 2000, ApJ, 538, L1
Morton, D. 2003, ApJS, 149, 205
Murray, N., Quataert, E., & Thompson, T. 2005, ApJ, 618, 569
Murray, N., Menard, B., & Thompson, T. 2010, arXiv:1005.4419
Overzier, R., Heckman, T., Schiminovich, D., Basu-Zych, A., Goncalves, T., Martin, D. C., & Rich, R. M. 2010, ApJ, 710, 979
Overzier, R., et al. 2008, ApJ, 677, 37
Overzier, R., et al. 2009, ApJ, 706, 203
Overzier, R., et al. 2011, ApJ, 726, L7
Pettini, M., Rix, S., Steidel, C., Adelberger, K., Hunt, M., & Shapley, A. 2002, ApJ, 569, 742
Putman, M., Bland-Hawthorn, J., Veilleux, S., Gibson, B., Freeman, K., & Maloney, P. 2003, ApJ, 597, 948
Quider, A., Pettini, M., Shapley, A., & Steidel, C. 2009, MNRAS, 398, 1263
Quider, A., Shapley, A., Pettini, M., Steidel, C., & Stark, D. 2010, MNRAS, 402, 1467
Razoumov, A., & Somer-Larson, J. 2010, ApJ, 710, 1239
Robert, C., Leitherer, C., & Heckman, T. 1993, ApJ, 418, 749
Robert, C., Pellerin, A., Aloisi, A., Leitherer, C., Hoopes, C., & Heckman, T. 2003, ApJS, 144, 21
Rupke, D., Veilleux, S., & Sanders, D. 2002, ApJ, 570, 588
Rupke, D., Veilleux, S., & Sanders, D. 2005, ApJ, 632, 751
Schwartz, C., Martin, C., Chandar, R., Leitherer, C., Heckman, T., & Oey, M. S. 2006, ApJ, 646, 858
Shapley, A., Steidel, C., Pettini, M., & Adelberger, K. 2003, ApJ, 588, 65
Shapley, A., Steidel, C., Pettini, M., Adelberger, K., & Erb, D. 2006, ApJ, 651, 688
Siana, B., et al. 2007, ApJ, 668, 62
Siana, B., et al. 2010, ApJ, 723, 241
Steidel, C., Erb, D., Shapley, A., Pettini, M., Reddy, N., Bogosavljevic, M., Rudie, G., & Rakic, O. 2010, ApJ, 717, 289
Steidel, C., Pettini, M., & Adelberger, K. 2001, ApJ, 546, 665
Tremonti, C., Moustakas, J., & Diamond-Stanic, A. 2007, ApJ, 663, 77
Vanzella, E., et al. 2010, ApJ, 725, 1011
Veilleux, S., Cecil, G., & Bland-Hawthorn, J. 2005, ARA&A, 43, 769
Verhamme, A., Schaerer, D., Atek, H., & Tapken, C. 2008, A&A, 491, 89
Verhamme, A., Schaerer, D., & Maselli, A. 2006, A&A, 460, 397
Walborn, N., Parker, J., & Nichols, J. 1995, VizieR On-line Data Catalog: III/188
Wang, B. 1995, ApJ, 444, 590
Wise, J., & Cen, R. 2009, ApJ, 693, 984